J Polym Environ (2013) 21:780–788
DOI 10.1007/s10924-013-0601-3

ORIGINAL PAPER

Green Composites of Poly (Lactic Acid) and Sugarcane Bagasse Residues from Bio-refinery Processes

Letian Wang · Zhaohui Tong · Lonnie O. Ingram · Qingzheng Cheng · Siobhan Matthews

Published online: 11 July 2013

Abstract Twin-screw extrusion was used to prepare the composites consisting of PLA and three types of sugarcane bagasse residues (up to 30 wt%) derived from different steps of a biorefinery process. Each residue had different composition, particle size and surface reactivity due to chemical and biological (enzyme, microbes) treatments that the biomass was subjected to. The effects of different residue characteristics on properties, crystallization behaviors and morphologies of PLA composites were investigated. Besides, a small amount (2 wt%) of coupling agent, Desmodur® VKS 20 (DVKS), was used to improve the interfacial bonding between PLA and bagasse residues. The results indicated that in the presence of 2 % DVKS, PLA composite with pretreated residue exhibited the maximum strength properties (98.94 % tensile strength and 93.91 % flexural strength of neat PLA), while PLA composite with fermentation residue exhibited the minimum strength properties (88.98 % tensile strength and 81.91 % flexural strength of neat PLA).

Keywords Sugarcane bagasse · Poly (lactic acid) · Composite · Twin-screw extrusion

L. Wang · Z. Tong (✉) · Q. Cheng
Department of Agriculture and Biological Engineering, IFAS, University of Florida, PO. Box 110570, Gainesville, FL 32611-0570, USA
e-mail: ztong@ufl.edu

L. O. Ingram
Department of Microbiology and Cell Science, University of Florida, PO. Box 110700, Gainesville, FL 32611, USA

S. Matthews
SCF Processing Ltd., Unit 65a, Boyne Business Park, Drogheda, County Louth, Ireland

Introduction

In recent years, there has been great interest in the use of bio-based materials derived from renewable resources due to concerns of the depletion of petroleum resources, greenhouse gas emission, and the environmental problems related to non-biodegradable petroleum-based materials. PLA is a hydrophobic thermoplastic polymer made from renewable agricultural feedstocks (corn starch) through fermentation followed by the polymerization of the lactic acid [1]. Because of its high strength and modulus, PLA has been a promising alternative to some petroleum-based polymer, which has been widely used in packaging, medical applications and automobile interior components [2, 3]. PLA's high cost is considered one of main obstacles for its lack of wide usage. The cost of PLA is not considered competitive in current US market. Unless its cost can be reduced from about $2 per lb to $0.40–0.80 per lb [4], its use in a greater number of applications will not occur. Many researchers have reported the enforcement of PLA by the incorporation of natural fibers such as jute fiber [5], flax fiber, kenaf fiber [3, 6–9] or lignocelluloses such as pine wood flour [10] and sweet beet pulp (SBP). The benefits of using natural fibers and lignocelluloses include their low cost, widespread availability, low density, biodegradability, high stiffness and better thermal stability [4, 6, 11, 12].

Sugarcane is one of the most important lignocellulosic biomass resources in the world as it can be used as a food resource (e.g. sugar and sugary food products) or feedstock to produce renewable fuels (e.g. ethanol) [13]. The current total global production of renewable fuels is 50 billion liters a year, about 40 % of which is derived from extracted sugarcane juice [14]. Meanwhile, the use of the sugarcane bagasse residue after sugar extraction to produce second-generation biofuel (e.g. ethanol) has been extensively studied recently

due to its wide-availability and low cost [15–18]. However, the process of using sugarcane bagasse residues to produce ethanol is not cost-effective due to high energy consumption required for a harsh pretreatment process, a complicated detoxification process and the use of expensive enzyme. This study aims to produce PLA composites by incorporating PLA and the low-cost residue from the bioethanol process (hard-to-hydrolyzed fibers and un-reacted lignin components) via twin screw extrusion. The use of hard-to-hydrolyzed residues is expected to not only reinforce the PLA composite but also allow a cost-effective bioethanol process by using mild pretreatment condition, generating less inhibitor, eliminating the expensive detoxification process and using less expensive enzyme.

To achieve this goal, in this work, PLA-based composites were prepared using a twin screw extruder followed by injection molding. Three types of sugarcane bagasse residues were used; the first was directly collected after the sugar extraction process, the second after pretreatment and the third after fermentation of a bioethanol process with a mild pretreatment process. During the bioethanol process, bagasse residues were subjected to chemical, physical or biological treatments (e.g. microbe, enzyme). These variations resulted in the residues of different compositions, surface activities, residue fiber quantities, and microstructures. In this study, we investigated the effects of bagasse residues that subject to different chemical, thermal and biological treatments in the bioethanol process on PLA composites' properties.

When incorporating hydrophilic fibers (or lignin) with hydrophobic PLA, the incompatibility between two materials results in insufficient interfacial bonding and undesirable mechanical properties of composites [7]. Interfacial bonding between fibrous additives and the polymer matrix significantly affects mechanical strength of composites [10, 12, 19–22]. The interfacial bonding could be improved through fiber surface modification by physical or chemical pretreatments [23, 24] and the use of coupling agents [6, 25]. It was reported that PLA composites incorporated with diluted sodium dioxide treated fibers had slightly improved tensile, impact and fracture properties while composites with steam exploded fibers showed very significant improvements in mechanical properties [26]. Isocyanate-type agents have been used as coupling agents in wood composites [27], natural fiber based composites [3], and PLA blends with bio-based additives including starch and sugar beet pulp [6]. In this study, a small amount of an isocyanate-type coupling agent Desmodur® VKS 20 (DVKS), a mixture of diphenylmethane-4,4′-diisocyanate (MDI), was used to improve the interfacial bonding of PLA with lignocellulosic residues. The effects of DVKS on properties and the molecular weight of PLA and its composites were examined in this study as well.

Materials and Experiments

Materials

Bagasse residues from different steps of a bioethanol process were collected, which included (1) Raw bagasse (RB): bagasse residues provided by Florida Crystals Corporation (Okeelanta, FL, USA) and used without further size reduction; (2) Pretreated bagasse (PB): the bagasse after a mild acid pretreatment (1 % w/w phosphoric acid solution, 4 h) and a steam explosion process (180 °C, 10 min); (3) Fermentation residue (FB): bagasse residue collected from the fermentation broth after a fermentation process at 37 °C for 144 h. All bagasse residues were washed with US standard test sieve #270 under warm tap water until effluent became clear and then dried in an oven at 70 °C for at least 24 h. The PLA 6202D pellets were purchased from NatureWorks LLC (Minnesota, USA). Desmodur® VKS 20 (DVKS), was generously provided by Bayer Material Science LLC (Leverkusen, Germany). It is a mixture of diphenylmethane-4,4′-diisocyanate (MDI) with isomers and higher functional homologues, which has a –NCO (isocyanate group) content of about 31.5 ± 1.0 %. Acetic acid (glacial, certified ACS), hydrogen peroxide (30 %, certified ACS), chloroform (HPLC grade) were purchased from fisher Scientific, USA.

Bagasse Residues Characteristics

Compositions of Bagasse Residues

Compositions of three types of bagasse residues (RB, PB and FB) were analyzed according to the National Renewable Energy Laboratory (NREL) method [28]. Monomer sugar contents after cellulose hydrolyzation were measured by High Pressure Liquid Chromatography (Agilent Technologies HPLC 1200 series, Santa Clara, CA, USA) equipped with BioRad Aminex HPX-87P ion exchange column (Hercules, CA, USA). The acid soluble lignin was determined by UV–Vis spectroscopy (Beckman DU800 UV/Vis Spectrophotometer, Brea, CA, USA). Both the acid insoluble lignin content and the ash content were obtained by gravimetric analysis. According to the NREL method [29], crude protein content was calculated from total nitrogen content, which was measured by Elementar vario MAX CNS elemental analyzer (Hanau, Germany).

Fiber Length Measurement for Bagasse Residues

A maceration method described by Franklin [30] was used to disintegrate the fiber bundles for the following fiber length analysis. In a maceration process, 99 % acetic acid and hydrogen peroxide with a volume ratio of 1:2 were

mixed together to form a maceration solution. Then 5 g of each bagasse sample was transferred into 150 mL of this solution and heated at 60 °C for 48-h reaction. After maceration, bagasse residues were washed extensively with DI water until a pH 7 was obtained. The fiber lengths of bagasse residues were measured by Fiber Quality analyzer (FQA, OpTest Equipments Inc, Hawkesbury, Ontario, Canada) at a consistency of 2 mg/L.

Composite Preparation

A co-rotating twin screw extruder (Prism TSE 24HC, Thermo Electron Corporation, Stone, UK), located at SCF Processing Ltd. (Drogheda, Ireland), and a pelletizer, was used to prepare the PLA/bagasse residue composites. The twin extruder has a screw diameter of 24 mm and a length to diameter ratio of 40:1. The extruder has ten temperature-controlled zones along its barrel as shown in Fig. 1. Table 1 lists the temperature profile from each zone. The screw speed of 100 rpm was used for all the experiments. Before extrusion, the PLA was dried at 80 °C for 2 h and the weight loss of the PLA before and after drying was noted at less than 3 wt%. The bagasse residues were also dried at 80 °C overnight in a vacuum oven and re-dried at 80 °C for 2 h in a convection oven immediately before processing. PLA, bagasse residues, and 2 wt% of coupling agent DVSK were pre-mixed in a blender and then the mixture was put in the extruder. After extrusion, the extrudate was cooled for 20 min and subsequently pelletized. The pellets were injection molded at melting temperature of 170 °C, injection pressure of 120 bars, and mold temperature of 38 °C at holding time of 2 min. The strips with the nominal dimensions of 100 × 12 × 4 mm were made.

Mechanical Properties Measurements

Tensile Test

Tensile test was performed on an Instron test frame with MTS renew package (model 1122, MA, USA) and the procedure were designed according to ASTM D 638-10 [31]. The frame was equipped with a 1,000 lb load cell and air grips for reproductive gripping. Each specimen was machined to type V shape and conditioned according to ASTM D 638 and ASTM 618 [32] respectively. Five replicates were tested for each specimen at a crosshead moving speed of 2 mm/min. Tensile strength (TS, strength at break), tensile elongation at break (TEB, cross head displacement) were recorded. Tensile elastic moduli of all composites were determined from the linear portion of stress–strain curves.

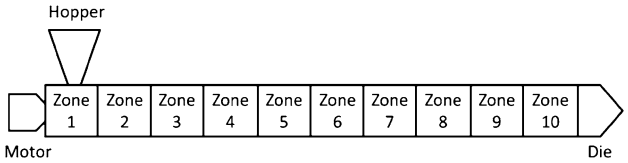

Fig. 1 Schematic diagram of the twin-screw extruder

Flexural Property Test

Flexural properties of pure PLA and its composites were measured according to ASTM D 790 [33] using an Instron testing machine (Model 5566, load cell capacity of 100N, Grove city, PA, USA) and conditioned as described in ASTM D 618. The nominal width and thickness are 12 and 4 mm, respectively. And the support span is 64 mm. Five replicates were tested for each specimen at a crosshead speed of 1.9 mm/min. Flexural modulus was the tangent modulus from the linear portion of stress–strain curves.

Thermal Analysis

The thermal behavior of PLA and its composites was analyzed by Differential Scanning Calorimeter (DSC 220C, Seiko instruments Inc, Japan). Samples were crimp sealed in 40-μL aluminum crucibles. All samples were first scanned from 25 to 190 °C at a heating rate of 10 °C/min to examine the glass transition, the cold crystallization and the melting temperature (T_g, T_{cc} and T_m) as well as their enthalpy changes (ΔH_{cc} and ΔH_m). After that, samples were kept at 190 °C for 5 min and then cooled to 25 °C at a cooling rate of 10 °C/min to study the non-isothermal melt crystallization temperature and enthalpy (T_{mc} and ΔH_{mc}). The heating and cooling cycles were repeated 3 times under constant gaseous nitrogen flow.

Molecular Weight Measurement

The molecular weight (Mw) of the PLA and its composites was measured by size exclusion chromatography (SEC), an Agilent Technologies 1260 series HPLC systems equipped with a refractive index detector (RID) and a multiple wavelength detector (MWD) (CA, USA). Three columns were connected in series including PLgel mixed B, PLgel

Table 1 Temperature profile of the twin extruder for composite processing

Zone	1	2	3	4	5	6	7	8	9	10	Die
Barrel temp. (°C)	30	155	160	165	165	162	164	165	165	160	165

mixed E 5 μm with a pore size of 10000A and PLgel mixed E 5 μm with a pore size of 100A. The PLA and its composite samples were dissolved in HPLC-grade chloroform for 8 h at a concentration of approximately 0.5 wt%. Then the solution was filtered through 0.22 μm syringe filter before injections to remove the un-dissolved materials such as cellulose and lignin. 50 μL filtered solution was injected in each run and thermostat temperature was set at 25 °C and the flow rate was 1 mL/min. All results were processed using ChemStation software package with GPC analysis (Rev.B.04.03). The molecular weight was calculated based on a universal calibration using a set of polystyrene standard.

Scanning Electron Microscopy

Scanning electron microscopy (SEM) (JOEL JSM-6400, operating voltage of 5–15 kV, JEOL, Peabody, MA, USA) was used to examine the morphologies of bagasse residues from different steps of the bioethanol process and the topographies of fracture surfaces of composites after tensile testing. All samples were coated with gold before scanning.

Statistical Analysis

Analysis of variance (ANOVA) was used to analyze the results of tensile tests, flexural tests and the molecular weight measurements. General linear model with a pairwise comparison, Tukey test under a 95 % confidence interval ($\alpha = 0.05$) in Minitab 16 software package was used.

Results and Discussions

Bagasse Residues Characteristics

Table 2 summarizes all the compositions and the average fiber lengths of bagasse residues (RB, PB and FB). The pretreated bagasse residues (PB) had the highest percentage of cellulose fibers because most hemicelluloses were broken down to soluble monomer sugars during pretreatment. This result agreed well with a lower percentage of hemicellulose in PB. The lignin content was increased and the fiber length was decreased with enhanced hydrolysis severity and progressive digestion of polysaccharides to monomer sugars during the bioethanol process. As shown in Table 2, the fiber length of PB was almost half of that of RB, while the fiber length of FB was approximately half of PB, which indicated that cellulose fiber chains were cut to shorter chains during the hydrolysis process. The residues (PB and FB) were collected by washing them under warm tap water on US standard test sieve #270 until effluent became clear. Soluble components (enzyme, dead cells, soluble lignin and original protein, approximately 15 wt%) and insoluble lignin components with a small particle size (approximately total 10 wt%) were lost in the filtrate, which resulted in a relatively high percentage of cellulose for PB (53.29 wt%) and FB (44.81 wt%) samples. The loss of relatively-large quantity of lignin is because that the sieve used for washing has large mesh opening size. Because residues are the aggregates with small particle sizes and high visocosity, the sieve with large mesh opening size was used to ensure the collection of plenty of residues for our experiment.

Figure 2 shows the morphologies of three types of bagasse residues. The raw bagasse (RB) was composed of fiber bundles with near-smooth surfaces without any significant surface fibrillation (Fig. 2a). In PB, fiber bundles disappeared and individual fiber layers with large surface areas and significant surface fibrillation were observed (Fig. 2b). The fermentation bagasse residues (FB) (Fig. 2c) were composed of large quantity of particles with a very low aspect ratio. As depicted in Table 2, these particles could consist of a large quantity of lignin particles and small amount of residue carbohydrates after most polysaccharides were hydrolyzed to monomer sugars, which were further converted to ethanol during bioethanol process.

Mechanical Properties

Tensile Properties

Figures 3 and 4 and Table 3 demonstrate tensile properties including tensile strength (TS), tensile elongation at break

Table 2 Composition and fiber characteristics of three types of bagasse residues: RB—the raw bagasse residues; PB—the pretreated bagasse residues; FB—the bagasse residues after fermentation

Material	Lignin %	Cellulose %	Hemicellulose %	Protein %	Ash %	Acetic acid %	Fiber length (mm)
RB	26.70	39.72	27.85	2.75	1.91	1.15	1.23
PB	29.33	53.29	14.90	1.43	1.05	0	0.63
FB	40.19	44.81	11.52	2.51	0.95	0	0.28

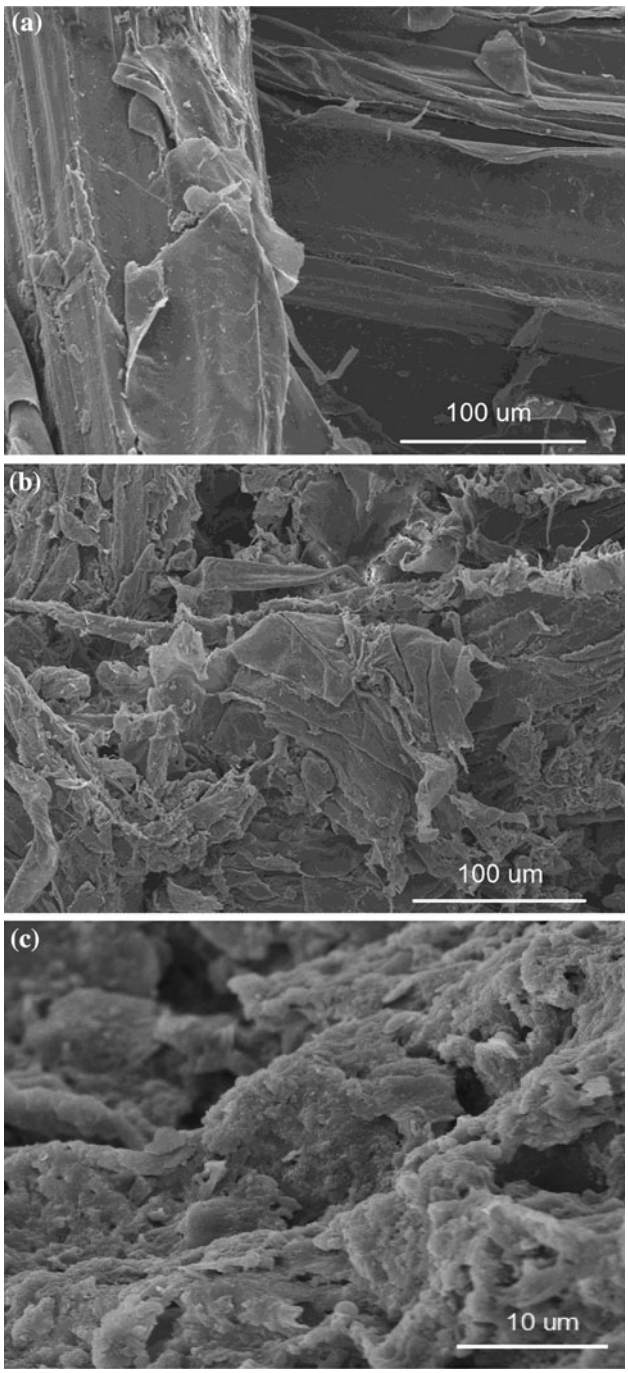

Fig. 2 SEM images of three types of bagasse residues **a** raw bagasse residues, RB (*scale* 100 μm); **b** pretreated bagasse residues, PB (*scale* 100 μm); **c** fermentation bagasse residues, FB (*scale* 10 μm)

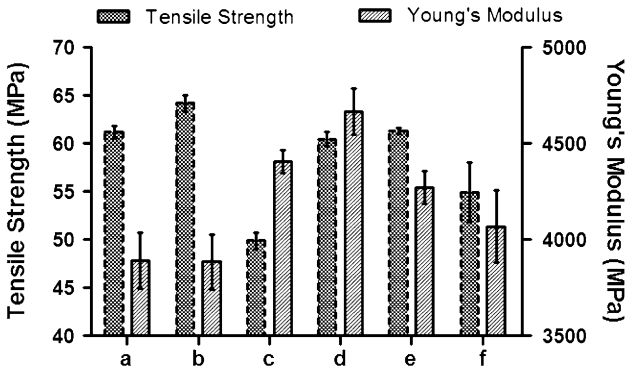

Fig. 3 Effect of three types of residues and DVKS on tensile strength and tensile elastic modulus of neat PLA and its composites. (*a* Neat PLA; *b* PLA with 2 % DVKS; *c* 70 % PLA, 30 % PB; *d* 70 % PLA, 30 % RB, 2 % DVKS; *e* 70 % PLA, 30 % PB, 2 % DVKS; *f* 70 % PLA, 30 % FB, 2 % DVKS)

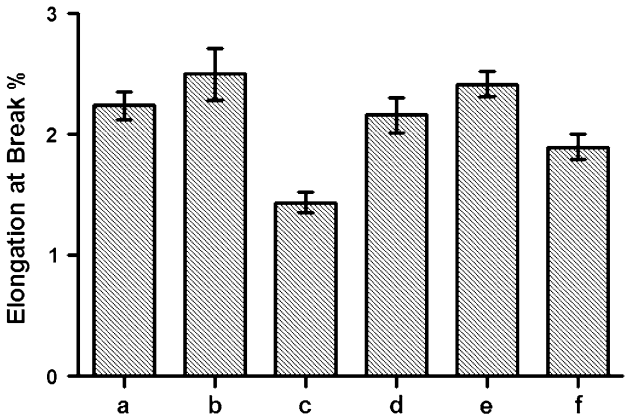

Fig. 4 Effect of three types of residues and DVKS on tensile elongation at break of neat PLA and its composites. (*a* Neat PLA; *b* PLA with 2 % DVKS; *c* 70 % PLA, 30 % PB; *d* 70 % PLA, 30 % RB, 2 % DVKS; *e* 70 % PLA, 30 % PB, 2 % DVKS; *f* 70 % PLA, 30 % FB, 2 % DVKS)

(TEB), tensile elastic modulus (TEM) for neat PLA, PLA with 2 wt% DVKS, PLA composites with the substitution of 30 wt% PB and PLA composites with the substitution of 30 wt% RB, PB and FB and in the addition of 2 wt% DVKS. ANOVA and Tukey method under 95 % confidence level were used to identify differences of tensile and flexural properties among different samples. Different letters in TM columns of Table 3 represent the significant difference in properties ($\alpha = 0.005$). For example, tensile properties shown in Table 3 indicated that the addition of DVKS didn't significantly affect the TS, TEB and TEM of neat PLA. However, the addition of pretreated bagasse residues without the coupling agent DVKS significantly decreased the TS and slightly increased the TEM (A/AB). This can be explained by the incompatibility between hydrophobic PLA and hydrophilic bagasse residues. Also, Residual bagasse tends to form agglomerates which could become the weak point in composites and causes early fracture [6]. However, the addition of 2 wt% coupling agent DVKS resumed TS and TEB of PLA composites with 30 % PB to 99 % and 116 % of neat PLA, respectively. It suggested that DVKS acted as a coupling agent

Table 3 Effect of different residues and DVKS on the mechanical properties of neat PLA and PLA composites

Sample	Tensile properties								Flexural Properties			
	TS (Mpa)	TM	TEB (%)	TM	TEM (Mpa)	TM	FS (Mpa)	TM	FEB (mm)	TM	FM (Mpa)	TM
a	62.0 ± 1.9	A	2.1 ± 0.1	AB	4,013.2 ± 271.8	A	104.0 ± 1.1	A	25.2 ± 3.1	A	1,816.3 ± 39.9	A
b	64.2 ± 1.9	A	2.5 ± 0.5	A	3,885.7 ± 321.1	A	105.3 ± 4.9	A	15.6 ± 1.91	B	1,753.6 ± 98.4	A
c	49.9 ± 1.9	B	1.4 ± 0.2	C	4,408.7 ± 134.8	AB	81.1 ± 1.5	B	6.36 ± 0.2	C	2,439.6 ± 28.8	B
d	60.5 ± 1.6	AC	2.2 ± 0.3	AB	4,668.3 ± 268.8	B	97.9 ± 2.0	A	8.3 ± 0.14	C	2,507.8 ± 49.2	B
e	61.4 ± 0.7	A	2.4 ± 0.2	AB	4,272.5 ± 193.5	AB	97.7 ± 9.8	A	8.9 ± 0.3	C	2,301.0 ± 225.7	B
f	54.9 ± 6.9	BC	1.9 ± 0.2	BC	4,069.1 ± 419.5	A	85.2 ± 2.7	B	7.2 ± 0.4	C	2,330.0 ± 55.1	B

TS tensile strength, *TM* Tukey method 95 % confidence interval, *TEB* tensile elongation at break, *TEM* tensile elastic modulus, *FS* flexure strength, *FEB* flexural elongation at break, *FM* flexural modulus

a, Neat PLA; b, PLA with 2 % DVKS; c, 70 % PLA 30 %PB; d, 70 % PLA, 30 % RB, 2 % DVKS; e, 70 % PLA, 30 % PB, 2 % DVKS; f, 70 % PLA, 30 % FB, 2 % DVKS

between bagasse residue and PLA because the –CNO group of DVKS could react with the surface hydrogen bonding, the residue water in bagasse residues and the carbonyl group of the PLA [25, 34].

The TS and the TEB of PLA composites with 30 % residues (RB and PB) substitution and in the addition of 2 % DVKS didn't exhibit significant difference with those of pure PLA. We observed that PLA composite with PB had higher TEB than the composite with RB even though RB had twice longer fiber length than PB. It indicated that more specific surface areas generated through chem-thermal pretreatment, which could provide more interfacial bonding between the PLA and the bagasse residue. FB exhibited the least reinforcing to PLA composites and the TS was significantly different with neat PLA. The TS, TEB and modulus of the PLA composite with FB were 88.58, 91.35 and 93.62 % of those of neat PLA, respectively. As we mentioned before, FB consisted of a large quantity of lignin particles with a low aspect ratio, which resulted in lower strength properties of the residue itself. The moduli of all the composites were higher than that of neat PLA, which suggested that the bagasse residue provided the additional nature of modulus in the PLA composite. This result agreed well with modulus results in the addition of lignocellulosic fillers [6].

Flexural Properties

As shown in Fig. 5 and Table 3, the effects of different residues and DVKS on the flexural strength (FS) and flexural modulus (FM) of PLA and its composites follow the similar trend as their effects on the tensile strength (TS) and tensile elastic modulus (TEM). As shown in Table 3, the addition of DVKS didn't significantly change the FS but decreased flexural modulus (FM) of neat PLA (78 % of neat PLA, $\alpha = 0.005$). We also observed that all the PLA composites had a significantly increased FM in comparison to pure PLA ($\alpha = 0.005$). High modulus indicated the efficient stress transfer between PLA and the filler, which led to a higher impact resistance of PLA composites in the addition of the coupling agent. As shown in Table 3, there was no significant difference in flexural strength (FS) of PLA composites with PB and RB and pure PLA in the presence of DVKS. However, the FS of PLA composite with FB was much lower than that of PLA composites with PB and RB ($\alpha = 0.005$).

Thermal Properties

Figure 6 shows DSC thermograms of PLA and its composite samples and Table 4 summaries all the DSC data shown in Fig. 6. While the addition of PB and DVKS individually decreased the glass transition temperature (T_g) of PLA polymer, T_g was in the same level of that of neat PLA when incorporating both PB and DSVK in the PLA matrix. The increase of Tg for PLA composites in the presence of both PB and coupling agent DSVK may be attributed to the confined polymer chain formed by interfacial reaction among bagasse hydroxyl groups, –NCO group of DVKS, and PLA carbonyl groups. The T_m of PLA composites and the PLA in the presence of DVKS were lower than that of neat PLA. It is because that DVKS has plasticization effects and lignin (main component of the residues) can also act as natural adhesives as previously reported [35]. The cold crystallization was observed for both the neat PLA and its composites. But the melt crystallization of neat PLA was undetectable in DSC thermograms. Neat PLA was not able to crystalize during the injection molding process. This could be caused by rapid cooling during the molding process. Melt crystallization was detected in all the PLA composites and the PLA in the presence of DVKS. PLA composites with PB and DVKS

exhibited maximum melting crystallization (maximun T_{mc} and ΔH_{mc}) because the maximum surface areas of this composite allowed more heteronucleation and growth of PLA crystals.

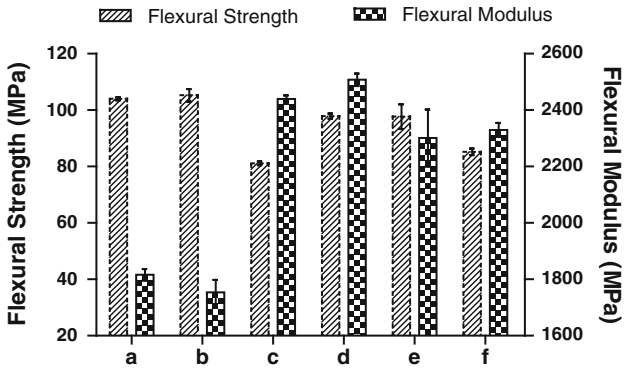

Fig. 5 Effect of three types of residues and DVKS on flexural strength and flexural modulus of neat PLA and its composites. (*a* Neat PLA; *b* PLA with 2 % DVKS; *c* 70 % PLA, 30 % PB; *d* 70 % PLA, 30 % RB, 2 % DVKS; *e* 70 % PLA, 30 % PB, 2 % DVKS; *f* 70 % PLA, 30 % FB, 2 % DVKS)

The Molecular Weight

The molecular weight (Mw) of the PLA and its composites measured by SEC are shown in Table 5. Without DVKS, bagasse residues greatly decreased the Mw of PLA. There are two reasons for this decrease. One reason is that hydrophobic PLA and hydrophilic residues are not compatible with each other. The second reason is that PLA may be hydrolyzed by the residue water and acetic acid in bagasse residues at high temperature [36–38]. In the presence of 2 % DVKS, the Mw of PLA was slightly increased. DVKS extended the PLA chain because that the isocyanate group of DVKS reacted with carbonyl group and hydroxyl group of PLA molecules [6]. Regarding PLA composites with different types of residues, PLA composites with PB had the highest molecular weight and the composite with RB had the lowest molecular weight. This result indicated that chain extending is directly correlated with the exposed surface areas. PB had the most exposed surfaces, which generated more active reaction sites to aid the formation of more bonding between PLA, the coupling agent and PB.

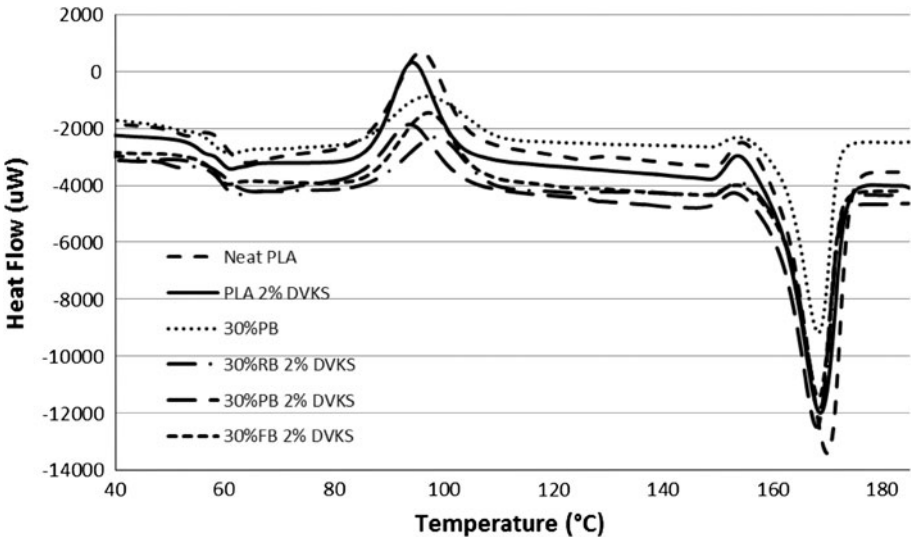

Fig. 6 DSC thermograms of neat PLA, PLA with 2 % DVKS and its composites (1st scan)

Table 4 Effect of three types of bagasse residues and DVKS on the thermal properties of neat PLA and its composites

	T_g (°C)	Cold crystallization		Melting		Melt crystallization	
		T_{cc} (°C)	ΔH_{cc} (J/g)	T_m (°C)	ΔH_m (J/g)	T_{mc} (°C)	ΔH_{mc} (J/g)
PLA 0 % DVKS	59.6	95.7	−21.7	169.9	47.7		
PLA 2 % DVKS	59.1	94.2	−20.9	168.7	45.4	110.3	−10.9
30 % PB	57	96.8	−17.2	168.3	34.7	95.6	−9.0
30 % RB 2 % DVKS	59.7	98.4	−14.7	168.5	31.5	112.3	−13.1
30 % PB 2 % DVKS	59.9	93.6	−13.7	167.9	31.7	115.3	−21.8
30 % FB 2 % DVKS	57.7	97.2	−17.6	168.3	31.3	110.8	−10.0

T_g, glass transition temperature; T_{cc}, cold crystallization temperature; ΔH_{cc}, enthalpy of cold crystallization; T_m, melting temperature; ΔH_m, enthalpy of melting; T_{mc}, temperature of melt crystallization; ΔH_{mc}, enthalpy of melt crystallization

Table 5 The molecular weight of neat PLA and its composites

Material	Mw	Mn	PDI
Neat PLA	1.16E+05	6.02E+04	1.92
PLA 2 % DVKS	1.17E+05	5.99E+04	1.96
70 % PLA 30 % PB	9.93E+04	5.24E+04	1.90
70 % PLA 30 % RB 2 % DVKS	1.09E+05	5.58E+04	1.95
70 % PLA 30 % PB 2 % DVKS	1.28E+05	7.01E+04	1.82
70 % PLA 30 % FB 2 % DVKS	1.25E+05	6.56E+04	1.91

Mw weight weighted molecular weight, *Mn* number weighted molecular weight, *PDI* polydispersity index

RB had an intact cell wall structure, which prevented the formation of inter-bonding and resulted in a low Mw. The strength of the PLA composite with RB mainly derived from the strength of fiber bundles themselves. FB also had some exposed areas due to the biological, chemical and mechanical treatments that it was subjected to. It had the molecular weight close to PB but higher than RB.

Morphologies of PLA and Its Composites

As shown in Fig. 7, the fractural surfaces of neat PLA and PLA composites were examined by SEM. The fracture surface of neat PLA was relatively smooth and uniform (Fig. 6a). In the presence of 30 % RB (Fig. 6b), intact fiber bundles were clearly shown in the plane. Some interstices were observed in the areas between the PLA and fibers, especially at the sites where fibers were pulling out of the plane during the tensile test. The intact fiber bundles could not provide more surfaces to facilitate inter-bonding between PLA and bagasse residues but had good mechanical strength by themselves. The fracture surfaces of PLA composites with PB and FB had no visible interstices, which could be caused by better inter-bonding between the PLA and fibrils. A large number of fibrils were clearly shown in the SEM image of PLA composite with PB, which resulted in better strength of this composite. The results agreed well with the previous analysis. Large quantity of lignin particles and the residue fibers with a low aspect ratio were seen in the PLA composite with FB.

Conclusions

In this study, twin-screw extrusion followed by injection molding was used to prepare green PLA composites with the substitution of three types of sugarcane bagasse residues (RB, PB and FB, 30 %). We first studied bagasse

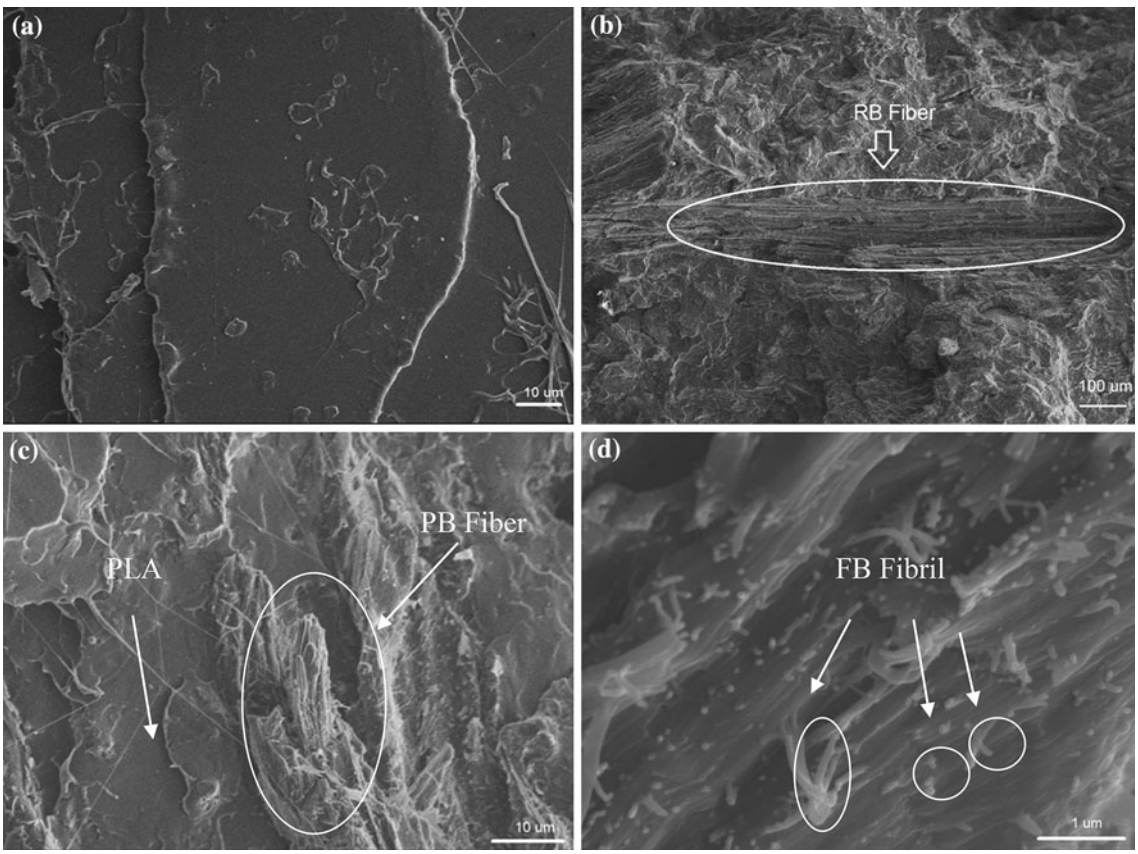

Fig. 7 SEM images of tensile fracture surfaces of **a** neat PLA; **b** PLA with 30 % RB and 2 % DVKS; **c** PLA composites with 30 % PB and 2 % DVKS; **d** PLA composite with 30 % FB and 2 % DVKS

residues' characteristics in terms of their components, residue fiber lengths and morphologies. The fiber length was gradually decreased (FB < PB < RB) and the lignin percentage was increased with the increased hydrolysis severity that residues were subjected to in the bioethanol process. Then we investigated the effects of these variables on mechanical and thermal properties, crystallization behavior and morphologies of PLA composites. The results demonstrated that the lignocellulosic residues increased the tensile and flexural moduli of PLA. In the aspect of mechanical properties, PLA composites with the substitution of 30 wt% of PB and 2 % DVKS showed the best mechanical strength (98.94 % tensile strength and 93.91 % flexural strength of neat PLA). The PLA composites with FB showed the least reinforcement (88.58 % tensile strength and 81.91 % flexural strength of neat PLA). The T_g of PLA composites followed the same trend as the tensile strength and T_m was slightly decreased in the presence of plasticizer DVKS and bagasse residues. In order to improve the inter-bonding between hydrophobic PLA and hydrophilic residues, a small amount of coupling agent (2 wt%, DVKS) was used and it extended the PLA molecular chain as depicted by a higher molecular weight. Finally, we could conclude that the properties of PLA composites were determined by multiple factors including residue fiber lengths, fiber aspect ratios, fiber quantities and the inter-bonding capability between the PLA and residues. Our future work will focus on further properties' improvement of composites through the approaches that improve the inter-bonding between biopolymer and residues. These approaches may include the use of more active coupling agent and the reduction of particle sizes of FB in a smaller scale (micrometer or nanometer scale).

Acknowledgments This project is supported by Biomass Research and Development Initiative Competitive Grant No. 2001-10006-3058 from the USDA National Institute of Food and Agriculture and Institute of Food and Agricultural Sciences (IFAS) Start-up funding at the University of Florid. The authors also thank the experimental help from Dr. C. Geddes, Dr. I. Nieves, Dr. Z. Fu, Mr. M. Mullinix at Bioethanol Pilot Plant, University of Florida; Dr. Y. Deng, Dept. of Chemical Engineering, Georgia Institute of Technology; Dr. A. Brennan, Dept. of Material Science and Engineering, University of Florida, Dr. Y. Li, Dept. of Soil and Water Science at Tropical Research and Education Center (TREC), University of Florida. The coupling agent DVKS provided by Bayer Material Sci, Germany is highly appreciated as well.

References

1. Lunt J (1998) Polym Degrad Stab 59:145
2. Auras R, Harte RB, Selke BS (2004) Macromol Biosci 4:835
3. Graupner N, Herrmann AS, Mussig J (2009) Compos A 40:810
4. Liu LS, Fishman ML, Hicks KB, Liu CK (2005) J Agric Food Chem 53:9017
5. Plackett D, Andersen TL, Pedersen WB, Nielsen L (2003) Compos Sci Technol 63:1287
6. Chen F, Liu LS, Cooke PH, Hicks KB, Zhang JW (2008) Ind Eng Chem Res 47:8667
7. Huda MS, Drzal LT, Misra M, Mohanty AK, Williams K, Mielewski DF (2005) Ind Eng Chem Res 44:5593
8. Ryntz RA (2006) J Coat Technol Res 3:3
9. John MJ, Thomas S (2008) Carbohydr Polym 71:343
10. Pilla S, Gong S, O'Neill E, Rowell RM, Krzysik AM (2008) Polym Eng Sci 48:578
11. Liu LS, Finkenstadt VL, Liu CK, Coffin DR, Willett JL, Fishman ML, Hicks KB (2007) J Biobased Mater Biol 1:323
12. Ochi S (2008) Mech Mater 40:446
13. Waclawovsky AJ, Sato PM, Lembke CG, Moore PH, Souza GM (2010) Plant Biotechnol J 8:263
14. Lam E, Shine J, Da Silva J, Lawton M, Bonos S, Calvino M, Carrer H, Silva-Filho MC, Glynn N, Helsel Z, Ma J, Richard E, Souza GM, Ming R (2009) GCB Bioenergy 1:251
15. Asghari A, Bothast RJ, Doran JB, Ingram LO (1996) J Ind Microbiol 16:42
16. Geddes CC, Peterson JJ, Roslander C, Zacchi G, Mullinnix MT, Shanmugam KT, Ingram LO (2010) Bioresour Technol 101:1851
17. Geddes CC, Mullinnix MT, Nieves IU, Peterson JJ, Hoffman RW, York SW, Yomano LP, Miller EN, Shanmugam KT, Ingram LO (2011) Bioresour Technol 102:2702
18. Patel MA, Ou MS, Ingram LO, Shanmugam KT (2005) Biotechnol Prog 21:1453
19. Pan PJ, Zhu B, Kai WH, Serizawa S, Iji M, Inoue Y (2007) J Appl Polym Sci 105:1511
20. Bax B, Muessig J (2008) Compos Sci Technol 68:1601
21. Ganster J, Fink HP (2006) Cellulose 13:271
22. Shibata M, Oyamada S, Kobayashi S, Yaginuma D (2004) J Appl Polym Sci 92:3857
23. Satyanarayana KG, Arizaga GGC, Wypych F (2009) Prog Polym Sci 34:982
24. Ibrahim NA, Yunus WMZW, Othman M, Abdan K (2011) J Reinf Plast Compos 30:38
25. Smith GD (2004) Wood Fiber Sci 36:228
26. Tokoro R, Vu DM, Okubo K, Tanaka T, Fujii T, Fujiura T (2008) J Mater Sci 43:775
27. Bao SC, Daunch WA, Sun YH, Rinaldi PL, Marcinko JJ, Phanopoulos C (2003) For Prod J 53:63
28. Sluiter AD, Hames BR, Ruiz RO, Scarlata C, Sluiter JB, Templeton DW, Crocker D (2008) NREL/TP-510-42618 determination of structural carbohydrates and lignin in biomass: laboratory analytical procedure, National Renewable Energy Laboratory
29. Hames BR, Scarlata CJ, Sluiter AD (2008) NREL/TP-510-42625 determination of protein content in biomass: laboratory analytical procedure (Revised) National Renewable Energy Laboratory
30. Franklin GL (1945) Nature 155:51
31. ASTM Standard D638-10 (2010) Standard test method for tensile properties of plastics
32. ASTM Standard D618-08 (2008) Standard practice for conditioning plastics for testing
33. ASTM Standard D790-03 (2003) Standard test methods for flexural properties of unreinforced and reinforced plastics and electrical insulating materials
34. Wang H, Sun XZ, Seib P (2001) J Appl Polym Sci 82:1761
35. Le Digabel F, Averous L (2006) Carbohydr Polym 66:537
36. Yang LX, Chen XS, Jing XB (2008) Polym Degrad Stabil 93:1923
37. Jung JH, Ree M, Kim H (2006) Catal Today 115:283
38. Felipe MGA, Vitolo M, Mancilha IM, Silva SS (1997) Biomass Bioenergy 13:11